Nephrol Dial Transplant (2009) 24: 85–96
doi: 10.1093/ndt/gfn433
Advance Access publication 11 September 2008

Original Article

NDT
Nephrology Dialysis Transplantation

Adventitial transplantation of blood outgrowth endothelial cells in porcine haemodialysis grafts alleviates hypoxia and decreases neointimal proliferation through a matrix metalloproteinase-9-mediated pathway—a pilot study

Deborah Hughes[1], Alex A. Fu[2], Alessandra Puggioni[3], James F. Glockner[2], Bilal Anwer[4], Antonio M. McGuire[5], Debabrata Mukhopadhyay[6] and Sanjay Misra[1,2,3]

[1]Division of Cardiovascular Diseases and Internal Medicine, [2]Department of Radiology, [3]Division of Vascular Surgery, Mayo Clinic, Rochester, [4]University of Minnesota Medical School, Minneapolis, [5]Mayo Medical School, Mayo Clinic, Rochester and [6]Department of Biochemistry and Molecular Biology, Mayo Clinic, Rochester, MN, USA

Abstract

Purpose. We hypothesized that adventitial transplantation of blood outgrowth endothelial cells (BOEC) to the vein-to-graft anastomosis of polytetrafluoroethylene grafts will reduce neointimal hyperplasia by reducing hypoxia inducible factor-1α (HIF-1α), by increasing angiogenesis in a porcine model of chronic renal insufficiency with haemodialysis polytetrafluoroethylene grafts. Because matrix metalloproteinases (MMPs) have been shown to be involved with angiogenesis, the expression of MMPs and their inhibitors was determined.

Methods. Chronic renal insufficiency was created by subtotal renal infarction and 28 days later, arteriovenous PTFE grafts were placed bilaterally from the carotid artery to the jugular vein. Autologous blood outgrowth endothelial cells labeled with *Lac Z* were transplanted to the adventitia of the vein-to-graft anastomosis using polyglycolic acid scaffolding and scaffolding only to other side (control). Animals were killed 14 days later and vessels were explanted from the vein-to-graft anastomosis of both sides and underwent immunohistochemical analysis, western blotting and zymography for HIF-1α, MMP-2, MMP-9, TIMP-1 and TIMP-2. BOEC were also made hypoxic and normoxic for 12, 24 and 48 h to determine protein expression for MMPs and TIMPs.

Results. Under hypoxia, BOEC significantly increased the expression of pro MMP-2 by 12 h and TIMP-2 by 24 h when compared to normoxic cells ($P < 0.05$). Transplantation of BOEC resulted in a significant decrease in both HIF-1α and intima-to-media ratio with a significant increase in both pro and active MMP-9 when compared to control vessels ($P < 0.05$). MMP-9 activity was localized to the neointima of the transplanted vessels by immunohistochemistry. There was increased CD31 density with engraftment of BOEC cells into the neointima of both the transplanted vessels compared to controls ($P = \text{NS}$).

Conclusion. Transplantation of BOEC resulted in a significant decrease in intimal hyperplasia and HIF-1α with a significant increase in both pro and active MMP-9 that was localized to the neointima of transplanted vessels. The increase in MMP-9 offers a possible mechanism for angiogenesis and the reduced intima-to-media ratio. Furthermore, we observed that BOEC had homed to the neointima of the contralateral vessels that had increased levels of HIF-1α, suggesting that hypoxia may be an important stimulus for BOEC migration.

Keywords: blood outgrowth endothelial cells; haemodialysis graft failure; hypoxia; restenosis; vascular biology

Introduction

In the United States, over half of the patients undergoing chronic haemodialysis require polytetrafluoroethylene (PTFE) grafts for vascular access [1]. The patency of PTFE haemodialysis grafts has been reported to be 50% at 1 year and 25% at 2 years [2]. Data suggest that haemodialysis vascular access graft failure results primarily from venous stenosis formation caused by intimal hyperplasia and subsequent thrombosis at the vein-to-graft anastomosis [3]. The intimal hyperplasia is composed of proliferating vascular smooth muscle cells with accompanying matrix deposition [4]. In patients with failed grafts, angiogenesis has been shown to occur within the neointima and adventitia along with increased expression of vascular endothelial growth factor (VEGF) and other growth factors [4]. These observations from clinical specimens suggest that angiogenesis plays an important role in haemodialysis vascular access

Correspondence and offprint requests to: Sanjay Misra, Department of Radiology, Mayo Clinic, 200 First Street SW, Rochester, MN 55905, USA. Tel: +1-507-255-7208; Fax: +1-507-255-7872; E-mail: misra.sanjay@mayo.edu

graft failure; however, the temporal sequence and exact nature of its relationship to intimal hyperplasia formation remains unclear.

Hypoxia is a fundamental stimulus for angiogenesis. It mediates gene expression of several important angiogenic factors through increased expression of hypoxia inducible factor-1 alpha (HIF-1α) including vascular endothelial growth factor-A (VEGF-A), vascular endothelial growth factor receptor-1 (VEGF-R1), matrix metalloproteinase-2 (MMP-2) and others [5]. A recent study from our laboratory showed that there was significantly increased expression of HIF-1α in tissue removed from the venous stenosis when compared to control veins in a porcine model of chronic renal insufficiency with arteriovenous PTFE haemodialysis grafts [6]. Moreover, in clinical specimens removed from patients with PTFE haemodialysis grafts, there was significantly increased expression of HIF-1α when compared to control veins [7]. Finally, there have been several studies in experimental animal models of atherosclerosis and arterial restenosis that have showed that there is increased hypoxia (HIF-1α) associated with the pathologic process [8]. Taken collectively, these data suggest a role for hypoxia (HIF-1α) in haemodialysis graft failure and alleviating hypoxia may help reduce intimal hyperplasia.

MMPs, specifically MMP-2 and MMP-9, and their endogenous inhibitors, tissue inhibitors of matrix metalloproteinases (TIMPs), play a key role in haemodialysis graft failure, vein graft remodeling [9] and angiogenesis [10]. Previous work from our laboratory has demonstrated early up-regulation of MMP-2, in a porcine model of haemodialysis vascular access graft failure that corresponded with increased cell migration from the adventitia to the media and intima leading to venous stenosis formation [9]. Reduced neointimal formation has been observed in experimental animal models with the use of non-specific MMP-2 and MMP-9 inhibitors [11]. We have shown that there is increased MMP-2 activity at the vein-to-graft anastomosis with subsequent increased expression of VEGF-R1 and TIMP-1 [9]. Furthermore, a recent laboratory study showed that in clinical specimens removed from patients with PTFE haemodialysis grafts, there was a significant increase in the expression of pro MMP-2, pro MMP-9 and TIMP-1 when compared to control veins [7]. In aggregate, these studies suggest a prominent role of MMPs in haemodialysis graft failure.

A recent study showed that in patients with end-stage renal disease, there is an imbalance between endothelial and smooth muscle progenitor cells [12]. It is hypothesized that this imbalance may explain the increased incidence of atherosclerotic cardiovascular disease in these patients [13]. Blood outgrowth endothelial cells (BOEC) are a subset of circulating progenitor cells that possess an endothelial cell phenotype [14]. They have been shown to have potential therapeutic effects in experimental animal models of restenosis after angioplasty [15] and neovascularization through MMP activation [16]. BOEC may be used to increase neovascularization by angiogenesis and thus reduce hypoxia. The aim of the present study was to determine the effect of hypoxia on BOEC and the production of MMPs and their inhibitors. Next, we determined whether transplanting BOEC to the adventitia of PTFE haemodialysis grafts would reduce venous stenosis formation and hypoxia by increasing angiogenesis in a porcine model with chronic renal insufficiency [17]. Because haemodialysis grafts are used in patients with advanced renal failure and the regulation of the targeted cytokines may be markedly different in the uraemic milieu, we performed these studies using a porcine model of renal insufficiency [6,17]. The expression of HIF-1α, MMP and TIMPs at the vein-to-graft anastomosis with immunohistochemical analysis was performed. Finally, luminal vessel area and blood flow were evaluated non-invasively by the use of magnetic resonance imaging and phase contrast magnetic resonance angiography (MRI/PC MRA).

Method and materials

Study design

BOEC were made either hypoxic or normoxic for 12, 24 and 48 h, and the production of HIF-1α, MMPs and TIMPs was determined. Seven castrated juvenile male pigs (40–50 kg, domestic swine, Larson Products, Sargeant, MN, USA) with chronic renal insufficiency induced by subtotal renal infarction were used [6,17]. In these animals, autologous BOEC were transplanted to the adventitia of the vein-to-graft anastomosis and the subsequent effect on vessel remodeling was examined in seven pigs with bilateral arteriovenous PTFE grafts. Prior to transplantation, autologous BOEC were stably transduced with a retrovirus carrying *Lac Z* for *in vivo* localization. As shown in Figure 1A, BOEC were seeded onto nanopore-sized scaffolding and wrapped around the adventitia of the vein-to-graft anastomosis at the time of graft placement, in contradistinction to the contralateral side that received only nanopore-sized scaffolding (control). Animals were subsequently followed for 14 days following graft placement. Luminal vessel area and graft patency were determined serially in each animal at Day 7, and Day 14 after graft placement using MRI and phase contrast MRA (Figure 1B) [9]. Animals were sacrificed at Day 14 and tissue specimens from the vein-to-graft anastomosis of the control and BOEC-transplanted veins were carefully examined to determine five aspects of graft pathology and pathophysiology: (1) relative levels of HIF-1α, MMP and TIMP expression; (2) identifying the location and ascertaining the quantity of BOEC engraftment; (3) angiogenesis using a semi-quantitative scoring method; (4) determination of the quantity of neointima formation; and (5) luminal vessel area and blood flow by non-invasive imaging using MRI. One animal was used for the three-dimensional microscopic computed tomographic analysis.

Appropriate Institutional Animal Care and Use Committee approval was obtained prior to performing any procedures on animals. In addition, housing and handling of the animals was performed in accordance with the Public Health Service Policy on Humane Care and Use of Laboratory Animals revised in 2000.

Anaesthesia

Prior to all procedures, animals were kept NPO (nothing per oral) for 12 h. They were initially anaesthetized

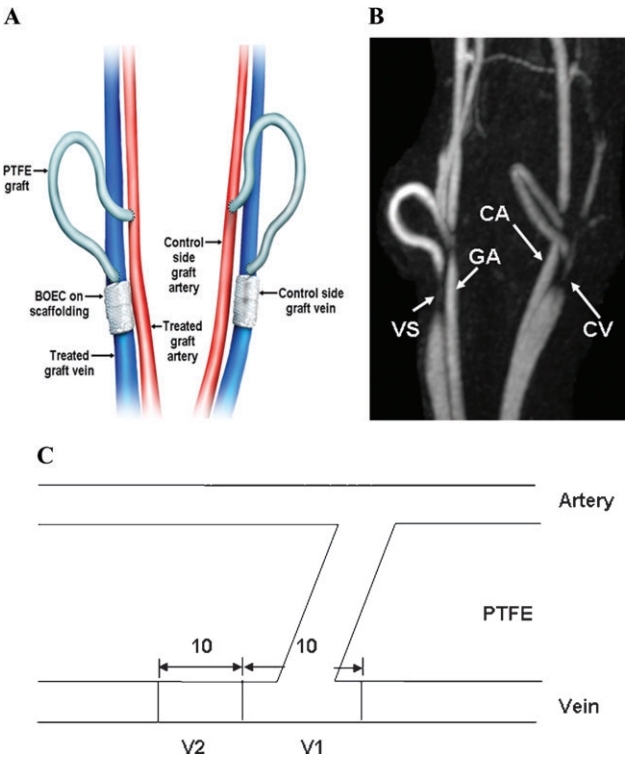

Fig. 1. Placement of polytetrafluoroethylene haemodialysis graft and representative MRI and PC MRA of venous stenoses. (**A**) Placement of polytetrafluoroethylene haemodialysis grafts. (**B**) MRI and PC MRA were performed in a Day 14 animal with BOEC treatment on the right (white arrow) and control on the left (yellow arrow). (**C**) Schematic showing the location of the vein-to-graft anastomosis used for histology (V1) and for protein analysis (V2). PTFE = polytetrafluoroethylene, VS = venous stenosis, GA = grafted artery, CA = control artery, CV = control vein.

with a combination of 5 mg/kg tiletamine hydrochloride (50 mg/mL) and zolazepam hydrochloride (50 mg/mL), 2 mg/kg xylazine (Bayer, Shawnee Mission, KS, USA) and 0.06 mg/kg glycopyrrolate given intramuscularly. To induce additional anaesthesia, an intravenous (IV) fluid line was placed in the ear vein for the delivery of zolazepam hydrochloride (5 mg/kg) which was also given as needed. During the procedure, the animals were intubated and placed on a positive-pressure ventilator delivering oxygen (3–5 mL/kg) and isoflurane (1–3%). The end-tidal CO_2 volume, oxygen saturation, heart rate, electrocardiogram and blood pressure were monitored throughout the surgical procedure.

Isolation and characterization of BOEC

Prior to renal artery embolization, 100 mL of blood was removed from the femoral artery of each pig. BOEC were isolated and expanded *ex vivo* as previously described, with some modifications [18]. Briefly, peripheral blood mononuclear cells were isolated by density gradient centrifugation with Ficoll-Paque Plus (Amersham Biosciences Corporation, Piscataway, NJ, USA). Red blood cells were lysed using a buffer containing 0.1 mM of EDTA, 10 mM of $KHCO_3$ and 150 mM of NH_4Cl. Next, mononuclear cells were washed with MCDB 131 medium (GIBCO Industries, Inc., Langley, OK, USA) supplemented with hydrocortisone (1 μg/mL, Sigma-Aldrich, St. Louis, MO, USA), cyclic-AMP (0.5 mM, EMD Biosciences, Inc., San Diego, CA, USA), amphotericin B (0.25 μg/mL, Sigma-Aldrich) and VEGF (10 ng/mL, R&D Systems, Minneapolis, MN, USA). Mononuclear cells were plated at a density of ~6×10^6 cells/well on six-well plates coated with rat tail Collagen type I (R&D Systems) in endothelial growth medium-2 (EGM-2, Cambrex Corp., Rutherford, NJ, USA).

The cell culture was maintained at 37°C, 5% CO_2 and 20% O_2. After 2 days, the media was changed and the non-adherent cells were removed. After satisfactory initial growth, the media was subsequently changed every 2–3 days. Between Days 15 and 18, colonies of cells appeared that exhibited typical endothelial morphology including a cobblestone pattern. Colonies were passaged and expanded for an additional 2 weeks. The adherent cells were harvested by trypsinization for transplantation.

The late outgrowth BOEC were characterized by a number of methods including endocytosis of acetylated low-density lipoprotein (acLDL) and expression of endothelial markers including VEGF-R2, von Willebrand factor (vWF), endothelial nitric oxide synthase (eNOS), caveolin-1 and CD-31. For uptake of acLDL, cells were incubated with acLDL (Molecular Probes, Invitrogen, Carlsbad, CA, USA) at a concentration of 10 μg/mL in EGM-2 for 4 h. Cells were washed with PBS and examined using fluorescent confocal microscopy at an absorption wavelength of 555 nm (acLDL).

Indirect immunofluorescence was performed to determine the expression of endothelial markers as follows. Briefly, cells were plated in Lab-TEK chamber slides and cultured at 37°C under normal culture conditions for 48 h or until cells were nearly confluent. Media was removed and cells were washed in warm PBS and then fixed in 4% paraformaldehyde for 15 min at 37°C for detection of extracellular antigen. For detection of intracellular antigens, cells were washed in cold methanol at 20°C for 15 min. Next, cells were blocked with a solution of 5% normal goat serum (NGS), 5% glycerol in PBS for 1 h at room temperature (RT). Tissue was incubated with a primary antibody suspended in PBS, 0.1% Tween 20, 0.1% bovine serum albumin (BSA) and Triton 0.1% for 1 h at RT. After incubation, cells were washed three times in PBS, followed by incubation with secondary antibody suspended in Tris buffered saline, with 0.1% Tween 20 (TBS-T) and 0.1% BSA. Cells were washed three times with PBS, followed by addition of mounting media containing DAPI (VECTA shield) and examined by conventional and confocal fluorescence microscopy.

The following antibodies were used: CD31 (Antigenix, Huntington Station, NY, USA, APG311, 1:100), CD14 (Antigenix, APG140, 1:10), CD45 (Antigenix, APG450-F, 1:10), α-smooth muscle actin (Lab Vision, Fremont, CA, USA, RB-9010, 1:100), e-NOS/NOS type III (BD Transduction Laboratories, San Diego, CA, USA, clone 3, 610296, 1:200) and caveolin (BD Transduction Laboratories, 610059, 1:200). The following secondary antibodies were used: goat anti-mouse Alexa-fluor 568 (Molecular probes, A-11004, 1:300), goat anti-rabbit (Molecular probes, A-11036, 1:200) and goat anti-rabbit FITC (Sigma-Aldrich, F-1262, 1:200).

BOEC protein expression in vitro under hypoxic conditions

To determine whether BOEC will secrete MMP proteins in response to hypoxia, BOEC were cultured under hypoxic and normoxic conditions for 12, 24 and 48 h. Briefly, BOEC were grown to 80% confluence and then placed in a water-jacketed CO_2 incubator that maintains a sub-ambient O_2 level (3%) by the regulated injection of N_2 (Hera Cell 150). Control cells were placed in a similar incubator that maintained the ambient O_2 level (20%). After the appropriate amount of time, cells were placed on ice and stimulation was halted by the addition of ice-cold PBS. Cells were washed three times with ice-cold PBS and lysed with a cold radioimmunoprecipitation buffer (20 mM Tris–HCl, pH 7.5, 0.15 MnCl, 1% Triton Z-100, 1 mM phenylmethylsulfonyl fluoride, 1 mM Na_3VO_4, 1 mM EDTA, 1 μg/mL leupeptin, 0.5% aprotinin and 2 μg/mL pepstatin A). Cell lysates and conditioned media were collected after centrifugation for 15 min at 4°C and stored at −80°C for western blot and zymographic analyses. Experiments were repeated three times.

Culture of BOEC and nanopore scaffolding

BOEC were cultured with the polyglycolic acid nanopore scaffolding prior to *in vivo* experiments to determine if there were any changes in cell morphology or growth characteristics. Briefly, porcine BOEC from passage 3 were seeded at a density of 2×10^4, plated onto collagen type I coated tissue in 12-well plates and cultured for 48 h in EGM-2 full growth media in the presence of sterilized 5 × 5 mm polyglycolic acid scaffolding. Control wells contained BOEC seeded at an equal density with EGM-2 only. After 24 h, cells were examined under light microscopy followed by trypsinization and counted with hemocytometer. Cell counts were reported as mean ± SD. Experiments were repeated in quadruplicate.

Preparation of retrovirus and transduction of BOEC

To allow for *in vivo* localization, BOEC were stably transduced with a retrovirus encoding *Lac Z*. Briefly, the retrovirus was prepared by seeding 293 T, human embryonal kidney cells at a density of $\sim 6 \times 10^6$ cells per 100 mm plate in 7 mL of full growth media containing DMEM (Mediatech Inc., Herndon, VA, USA) with 10% fetal bovine serum and 1× penicillin/streptomycin. DNA transfection was carried out using the effectene TM transfection reagent kit (Qiagen, Valencia, CA, USA). For each 100 mm plate, 2 mg of pMMp-*LacZ*, 1.5 mg of PMD.MLV gag.pol and 0.5 mg of pMD.G DNA that encode the cDNAs of the proteins required for viral packaging were mixed in 300 mL of Buffer EC (Qiagen, Valencia, CA, USA). Thirty-two microliters of enhancer (Qiagen, Valencia, CA) was added to the DNA mixture and incubated at RT for 2 min. Next 30 μL of effectene was added to the mixture, followed by 10-min incubation at RT. To this, 2.6 mL of full growth media was added. The DNA/media mixture was added in a dropwise fashion to each plate of 293T cells. The medium was changed after 16 h. The retrovirus was isolated 48 h after transfection and used immediately or frozen for future use at −80°C. Three days prior to surgical transplantation of cells, BOEC from passage 3 or 4 were seeded onto T125 flasks and grown to 50% confluence. For viral transduction, 8 mL of reduced media, containing EBM, 0.1% FBS, 1× penicillin/ampicillin and 10 ng/mL of VEGF, 8 mL of viral solution, 10 mg/mL of polybrene was added to each flask. After 8 h, an additional 15 mL of full growth media (EGM-2) was added, followed by a change in media after 16 h.

Creation of chronic renal insufficiency by renal artery embolization

Chronic renal insufficiency was created by subtotal renal infarction embolizing the renal artery as previously described [6,17,20].

PTFE graft placement

Haemodialysis grafts were placed as previously described with the following modifications [6,9,20]. Twenty-eight days after the renal artery embolization procedure, bilateral arteriovenous PTFE graft (4 mm diameter by 7 cm long, Gore, Flagstaff, AZ, USA) were placed from either the right or left carotid artery to the ipsilateral jugular vein (Figure 1A). On the ipsilateral vein-to-graft anastomosis, BOEC were seeded onto polyglycolic acid scaffolding (see later) that was placed around the adventitia while the contralateral side received polyglycolic acid scaffolding alone (control). These animals were killed at 14 days and the bilateral grafts with accompanying artery and vein were snap frozen in liquid nitrogen and stored at −80°C for Western blotting, zymography and histological analyses. One day prior to graft placement, all animals were given anti-platelet therapy by using Plavix (75 mg, Clopidogrel bisulfate, Sanofi-Aventis, Bridgewater, NJ, USA) by mouth that was continued until completion of the study. One day before graft placement and for 5 days after graft placement, the pigs were given antibiotics to prevent infection as previously described [9,17,19].

Adventitial transplantation of BOEC

To insure effective delivery of BOEC to the adventitia, we used a polyglycolic acid nanopore scaffolding that had BOEC seeded onto it directly as described by Godbey *et al*. [21]. The polyglycolic acid scaffolding was prepared from a density of 64 mg/cm^3, porosity of 95% and a thickness of 2.5 mm as previously described [21]. At the time of graft placement, BOEC, which were previously transfected with *Lac Z* retrovirus 3–4 days earlier, were removed by trypsinization and counted. Five million BOEC cells were suspended in 500 μL of EGM-2. This mixture was seeded directly onto the sterile 15 × 10 mm polyglycolic acid scaffolding, and then sutured loosely around the adventitia of the vein-to-graft anastomosis. On the contralateral side to serve as a control, scaffolding with 500 μL of EGM-2 was absorbed onto the inner surface and loosely sutured around the adventitia of the vein-to-graft anastomosis (Figure 1A).

Cine phase-contrast magnetic resonance imaging and contrast-enhanced magnetic resonance angiography (PC MRI/MRA)

To assess vascular remodeling of the BOEC-transplanted vessels and control vessels, MRI was performed as described previously, at the vein-to-graft anastomosis of BOEC-transplanted and control vessels [9,20,22]. MRI was performed serially in all animals at 7 and 14 days following graft placement. Luminal vessel area, blood flow and graft patency were determined using MRI. Our laboratory has used MRI in the past and the accuracy and reproducibility of MRI for measuring blood flow and area are described elsewhere [9,20,22]

Vessel harvesting

The vein-to-graft anastomosis, ∼2 cm proximal and cephalad to the stenosis, was removed as previously described [6,9,21]. These specimens were snap frozen in liquid nitrogen and stored at −80°C for subsequent western blotting, zymography and immunohistochemical analysis.

Western blot and SDS-PAGE zymography

To assess angiogenesis and MMP expression, we used Western blotting and zymography on whole tissue lysate, cell lysate and conditioned media as previously described. One hundred micrograms of protein (tissue) and 15 μg of cell lysate were used. Immunoreactive signals were detected by ECL methods (Amersham Pharmacia Biotech, Piscataway, NJ, USA) following the manufacturers instructions. Antibodies and antisera used included: HIF-1α (Novus Biochemicals, Littleton, CO, USA, Mouse anti-human), VEGF-A (Santa Cruz Biotechnology, SC-7269, Mouse anti-human), VEGF-R1 [Santa Cruz Biotechnology, SC-504, Rabbit anti-human (C-1158), LotG1505], VEGF-R2 [Santa Cruz Biotechnology, SC-316, Lot F2204, Rabbit anti-human (C-17)], TIMP-1 (R&D Systems, Clone no. 63515, Mouse IgG2B) and TIMP-2 (R&D Systems, Clone no. 127711, Mouse IgG1). Zymography was performed on whole tissue lysate, cell lysate and conditioned media as previously described [9,20].

Histological and morphometric analysis

To quantify the intima-to-media ratio, haematoxylin and eosin (H & E) and Verhoeff's van Giesen (VVG) staining were performed on 5-μm frozen sections on the vein-to-graft anastomosis as previously described [9,20]. Sections were obtained from the vein-to-graft anastomosis as shown in Figure 1C. Care was taken to include the cushioning and shoulder regions. Ten contiguous axial sections were obtained so that the lumen of the vein-to-graft anastomosis was circular and the average value of all 10 readings per animal was used [9,20,23]. To determine the location and degree of engraftment of the BOEC, frozen slides were stained for β-gal (beta-Gal, Stratagene, La Jolla, CA, USA) according to manufacturer's instructions. Fifteen sample sections from the vein-to-graft anastomosis of both the control and BOEC-transplanted vessels were stained for β-gal. Indirect immunofluorescence was performed for CD31, eNOS, α-smooth muscle actin, MMP-2 and MMP-9.

Quantitative image analysis

Sections stained for β-gal, CD31 and VVG stains were quantified as previously described [9,19]. For β-gal index, the entire neointima or normal intima was selected interactively; the area of *Lac Z*-positive (blue) was captured, by setting the appropriate RGB (red–green–blue) color intensity threshold. The β-gal index was obtained by calculating the area of positive β-gal over the total area of the neointima or intima. The neointima and intima were determined from the VVG-stained sections as previously described [9,19].

Adventitial angiogenesis

The amount of adventitial angiogenesis was quantified using the CD31 index. This was calculated by counting the number of positive CD31 cells per area/total cell number of cells per area in the adventitia adjacent to media, using the interactive KS 400 image analysis software as described previously [9]. This was blinded to prevent observer bias, and repeated twice to ensure that intraobserver variability was <10%. For each animal with a patent graft, the CD31 index in the adventitia, adjacent to the media, at the vein-to-graft anastomosis was measured from the BOEC-transplanted and non-transplanted vessels.

Three-dimensional microscopic computed tomography preparation and procedure

Three-dimensional microscopic computed tomography was performed in order to determine if the vasa vasorum of the jugular vein communicates with the vasa vasorum of the carotid artery as previously described [24]. A 6-cm section of carotid artery and the accompanying jugular vein were excised from a pig. A cannula was introduced into the carotid artery and heparinized saline was infused to clear any remaining blood from the vasculature. Microfil, a radiopaque polymer, was infused into the artery at a pressure of 100 mmHg and the distal end of the artery was clamped. The pressure was maintained until the polymer set. The sample was then fixed in 10% formalin. The microfil was removed from the lumen of the carotid artery; the specimen was encased in paraffin and then scanned using microscopic computed tomography as previously described [24].

Statistical methods

The luminal vessel area was obtained from the phase-contrast MRI with MRA and averaged for each time point for the vessels and for the cardiac cycle for each animal. Values are expressed as mean ± standard deviation (SD). Paired *t*-tests were used to compare the BOEC and control sides of the vessel. A P value ≤ 0.05 was considered statistically significant. SAS version 9 (SAS Institute Inc., Cary, NC, USA) was used for statistical analyses.

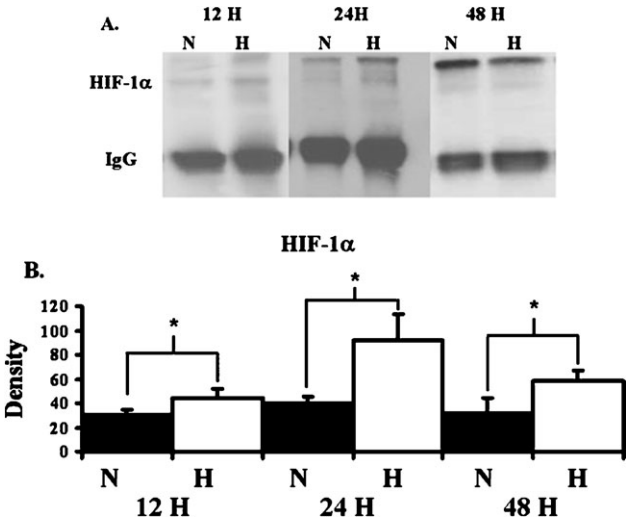

Fig. 2. HIF-1α expression as a function of time in the BOEC cells during hypoxia at different time points. (**A**) Graph (upper) representing appropriate protein band of HIF-1α from Western blot analysis and graph (lower) representing appropriate band for IgG from Western blot for protein loading. **N** is normoxia and H is hypoxia. (**B**) Semiquantitative analysis for HIF-1α performed at 12, 24 and 48 h. The normalized density of HIF-1α was significantly higher in hypoxic specimens when compared to normoxic specimens at all time points. ∗A significantly higher value ($P < 0.05$). Data are mean ± SD.

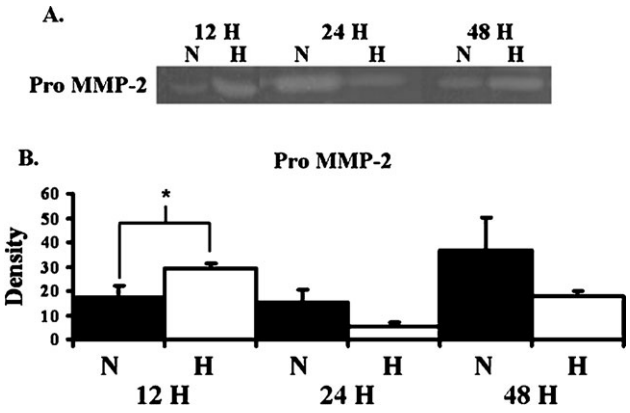

Fig. 3. Pro MMP-2 expression by BOEC under hypoxic conditions at different time points. (**A**) Graph (upper) representing appropriate protein band of pro MMP-2 from zymographic analysis. **N** is normoxia and H is hypoxia. (**B**) Semiquantitative analysis for HIF-1α performed at 12, 24 and 48 h. The normalized density of pro MMP-2 was significantly higher in hypoxic specimens when compared to normoxic specimens at 12 h. *A significantly higher value ($P < 0.05$). Data are mean ± SD.

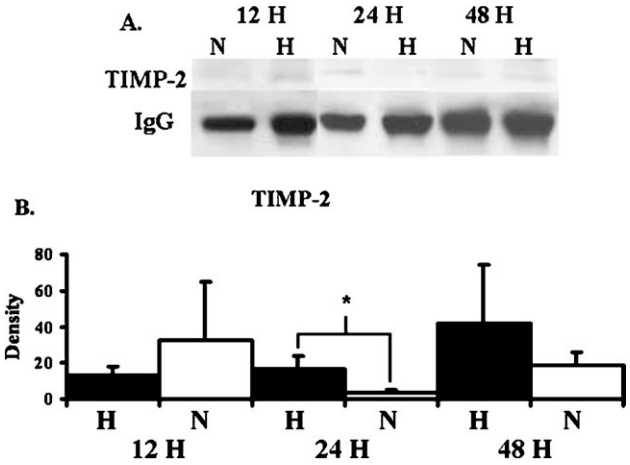

Fig. 4. TIMP-2 expression by BOEC under hypoxic conditions at different time points. (**A**) Graph (upper) representing appropriate protein band of TIMP-2 from Western blot analysis and graph (lower) representing appropriate band for IgG from Western blot for protein loading. **N** is normoxia and H is hypoxia. (**B**) Semiquantitative analysis for TIMP-2 performed at 12, 24 and 48 h. The normalized density of TIMP-2 was significantly higher in hypoxic specimens when compared to normoxic specimens at 12 h. *A significantly higher value ($P < 0.05$). Data are mean ± SD.

Results

Characterization of BOEC and culture with scaffolding

BOEC colonies appeared between Days 15 and 18 and exhibited the typical 'cobblestone' appearance of endothelial cells. Cells demonstrated uptake of acetylated LDL and stained positive for CD31, vWF, eNOS and caveolin-1. They were negative for CD14 and α-SMA. Cell population purity was estimated to be 95%. After 48 h of culture of BOEC with nanopore scaffolding, cells maintained their endothelial morphology. Cell doubling was 3.28 ± 1.6 and 2.88 ± 1.4 for control and nanopore scaffolding, respectively, indicating that the nanopore scaffolding had no significant effect on cell-doubling times.

Protein expression of hypoxic and normoxic BOEC

To assess the effects of hypoxia on protein production by BOEC, BOEC from passage 3 were harvested. Significantly increased amount of HIF-1α was observed in hypoxic BOEC when compared to normoxic BOEC at 12, 24 and 48 h (Figure 2, $P < 0.05$). By 12 h, BOEC produced significantly increased amounts of pro MMP-2 when compared to normoxic BOEC (Figure 3, $P < 0.05$). No active MMP-2 or MMP-9 was observed. There was a significant increase in the production of TIMP-2 by BOEC at 12 h when compared to normoxic BOEC (Figure 4, $P < 0.05$). No difference in TIMP-1 expression was observed at any of the time points. These results suggest that hypoxia may be an important stimulus for up-regulation of pro MMP-2 and TIMP-2 in BOEC.

Surgical outcomes

Seven castrated juvenile male pigs weighing 48.6 ± 1.2 kg underwent total embolization of the left kidney (7) and partial embolization of the right kidney (2 upper pole and 5 lower poles) using 150- to 250-μm polyvinyl acrylide particles in all animals. There were no complications as a result of the embolization procedure other than the expected induction of renal insufficiency. The average BUN and creatinine was 19.6 mg/dL and 2.78 mg/dL, respectively. The normal BUN is 6–21 mg/dL and creatinine is 0.8–1.2 mg/dL. Five pigs had bilateral placement of PTFE grafts. BOEC were transplanted on the right in one pig and

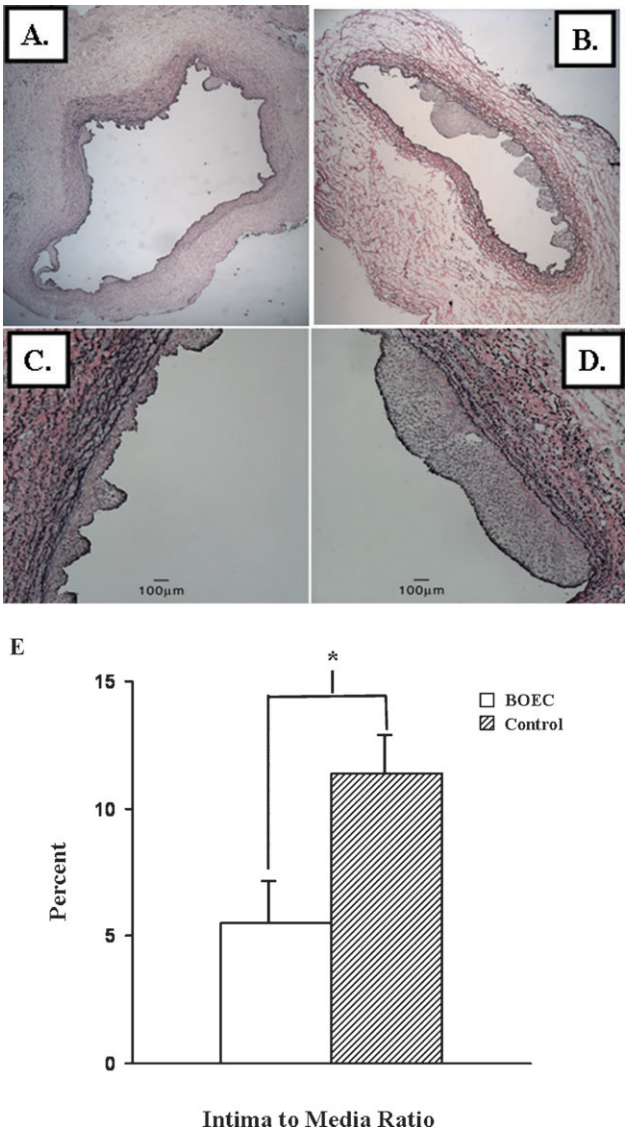

Fig. 5. Verhoeff's van Giesen staining was performed at the venous stenosis (section V1, see Figure 1C) from the cushioning region of the BOEC-transplanted (**A** and **C**) and contralateral non-transplanted (control) veins (**B** and **D**). **A** and **B** are 5× and **C** and **D** are 40× magnification. The lower panel (**E**) shows that there was a 50% decrease in the intima-to-media ratio in the BOEC-transplanted samples when compared to controls ($P < 0.05$). Data are mean ± SD.

on the left in four pigs with the contralateral vessels serving as controls (Figure 1A and B). To determine the effects of the nanopore scaffolding on protein expression, two pigs had bilateral PTFE grafts placed with nanopore scaffolding with *Lac Z* virus alone wrapped around the adventitia of the vein-to-graft anastomosis.

Histological and morphometric analysis

Examination of the VVG-stained vein-to-graft anastomosis removed from the BOEC-transplanted vessels revealed a decrease in the neointima (Figure 5A) when compared to the contralateral non-transplanted (control) vessels (Figure 5B). The intima-to-media ratio was determined for the vein-to-graft anastomosis of both BOEC-transplanted and non-transplanted vessels. The mean intima-to-media ratio of the transplanted BOEC vessels (5.5 ± 1.8) was 50% less than the control (11.4 ± 2.2, $P < 0.05$). Several important observations were made (Figure 5C). Examination of the adventitia at high-powered magnification (20×) revealed that the nanopore scaffolding was partially degraded with individual fibres found in the outermost adventitial layer. There was no evidence of inflammatory cells with the exception of an occasional giant cell (macrophage) seen in areas with degraded scaffolding.

Microvessels were seen primarily in the adventitia of the BOEC-transplanted vessels and contralateral non-transplanted (control) vessels, occasionally in the intima and rarely in the media (Figure 6A). Immunostaining was performed to determine the cell phenotype of the adventitial microvessels. This revealed that the cells were positive for both CD31 (Figure 6A) and eNOS (Figure 6D) and α-SMA. The neointima of both grafts was composed primarily of α-SMA cells with the rare CD31-positive cells (Figure 6A-B). Normal vein is shown for comparison (Figure 6C and E). In general, the presence of microvessels appeared more frequently in areas adjacent to neointima, as opposed to normal intima. These findings indicate that maturing blood vessel formation had occurred within the 14-day period.

To quantify the degree of angiogenesis, the number of CD31-positive cells was determined per high-power field (20×) for both the BOEC-transplanted (Figure 7A) and the contralateral non-transplanted (control) vessels (Figure 7B). The CD31 density was slightly higher in the adventitia of BOEC-transplanted vessels (0.17 ± 0.02) when compared to the contralateral non-transplanted (control) vessels (0.13 ± 0.03, $P = 0.12$, Figure 7C). These changes suggest that transplantation of BOEC enhances angiogenesis.

Engraftment of BOEC in the vessel wall was determined by beta-galactosidase staining for *Lac Z*. *Lac Z*-positive cells were observed in <1% of the adventitial microvessels of the BOEC-transplanted vessels (Figure 8A), with no *Lac Z*-positive cells in the adventitia of the contralateral non-transplanted (control) vessels (Figure 8B). In addition, *Lac Z*-positive cells were observed in both the neointima and intima of the BOEC-transplanted vessels (Figure 8A) and contralateral non-transplanted (control) vessels (Figure 8B). Engraftment of BOEC was twofold higher in the neointima and intima of the contralateral non-transplanted (control) vessel when compared to the ipsilateral BOEC-transplanted neointima and intima (Figure 8C). Although this may be important, statistical significance was not observed possibly due to the small sample size and low degree of engraftment. No *Lac Z*-positive cells were seen in the media. No *Lac Z*-positive cells were observed in the carotid artery of both vessels. We interpreted these results to indicate that the transplanted BOEC may have gained access to the systemic circulation in one of two ways: (i) they may have migrated through the media and intima of the transplanted vessel or (ii) they may have accessed the systemic circulation through the vasa vasorum of the vein that communicates with the arterial vasa vasorum (see later).

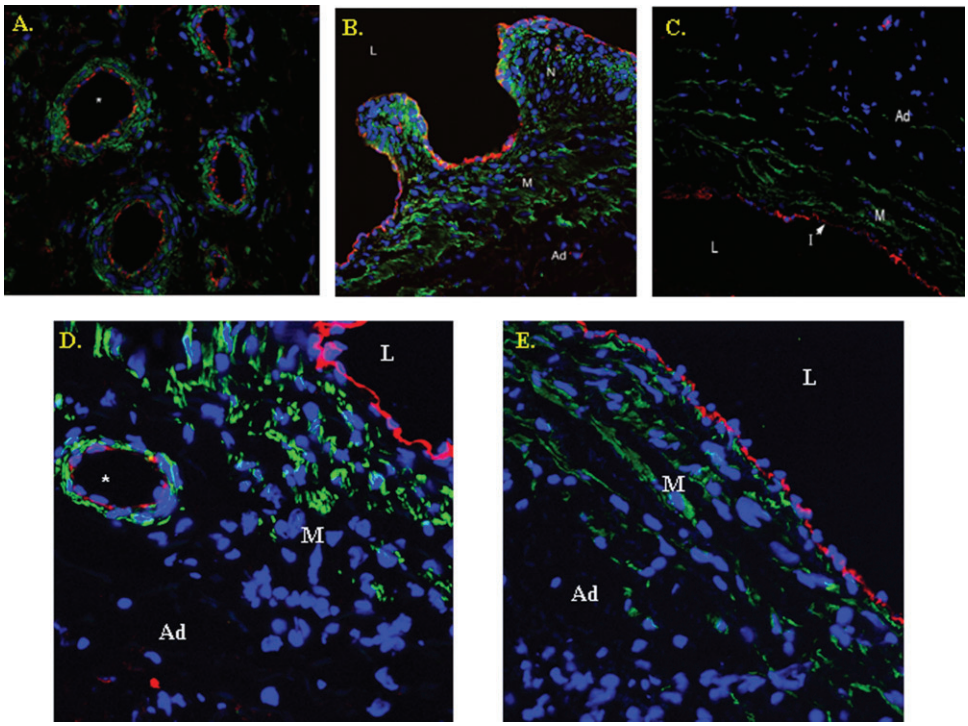

Fig. 6. Confocal triple immunostaining of the vein-to-graft anastomosis with transplanted BOEC from a Day 14 animal (**A**,**B**). For comparison, (**C**) is a normal vein. Blue denotes cell nuclei, green α-SMA and red CD31-positive cells. **A** shows that CD31-positive cells are lining the adventitial microvessels (*) surrounded by α-SMA-positive cells. **(B)** The neointima is composed primarily of α-SMA-positive cells. Ad is the adventitia, M is the media, N is the neointima and L is the lumen. For comparison, normal vein is shown in C. L is the lumen, I is the intima and M is the media. (**D**) A confocal double immunostaining of eNOS-positive cells (red) from BOEC-transplanted vessels. (**E**) A normal vein for comparison.

Temporal protein expression of the vein-to-graft anastomosis

The average HIF-1α expression (Figure 9A and C) decreased significantly in the transplanted BOEC vessels when compared to the contralateral non-transplanted (control) vessels ($P = 0.0475$). There was a significant increase in pro MMP-9 ($P = 0.043$) and a significant increase in active MMP-9 activity ($P = 0.05$, Figure 9B and C) in transplanted BOEC vessels when compared to the contralateral non-transplanted (control) vessels. No significant differences in pro MMP-2, active MMP-2, TIMP-1 and TIMP-2 were observed. In the four grafts removed from the two animals with only nanopore scaffolding and *Lac Z* virus placed around the vein-to-graft anastomosis, only pro MMP-9 was observed with no active MMP-9. These findings suggest that activation of MMP-9 was not due to the presence of scaffolding but resulted from the transplantation of the BOEC. Tissue immunostaining was performed with an antibody that recognized both the pro and active MMP-9. This revealed positive staining in the adventitial microvessels (Figure 9D). The highest degree of staining was in the neointima (Figure 9E) of both the BOEC-transplanted and non-transplanted (control) vein (Figure 9F) with a slightly higher degree of positive staining in the BOEC-transplanted vein. Overall, these results show that the major difference in protein expression between non-transplanted and BOEC-transplanted vessels is the presence of active MMP-9.

Luminal vessel area measurements by MRI

MRI was performed to determine the luminal vessel area of the vessels over time in the animals. The mean luminal vessel area for the BOEC-transplanted vessels was higher for all subsequent time points (P = NS). There was no difference in the blood flow between the transplanted BOEC and control vessels.

Three-dimensional microscopic computed tomographic imaging analysis

Three-dimensional microscopic computed tomographic analysis was performed on intact carotid artery and jugular vein to determine if the vasa vasorum of the jugular vein communicates with that of the carotid artery as it does in the coronary circulation [25]. This revealed a diffuse network of vasa vasorum that allowed for the passage of microfil from the arterial lumen into the adjacent venous lumen. The observation that *Lac Z*-positive BOEC cells were observed by Day 14 in both the neointima of the vein-to-graft anastomosis of the ipsilateral transplanted BOEC and the contralateral transplanted vessels raises the possibility that the BOEC may have gained access to the systemic blood supply (circulating) and homing to the neointima. Three-dimensional microscopic computed tomographic analyses demonstrated that the vasa vasorum is a possible route by

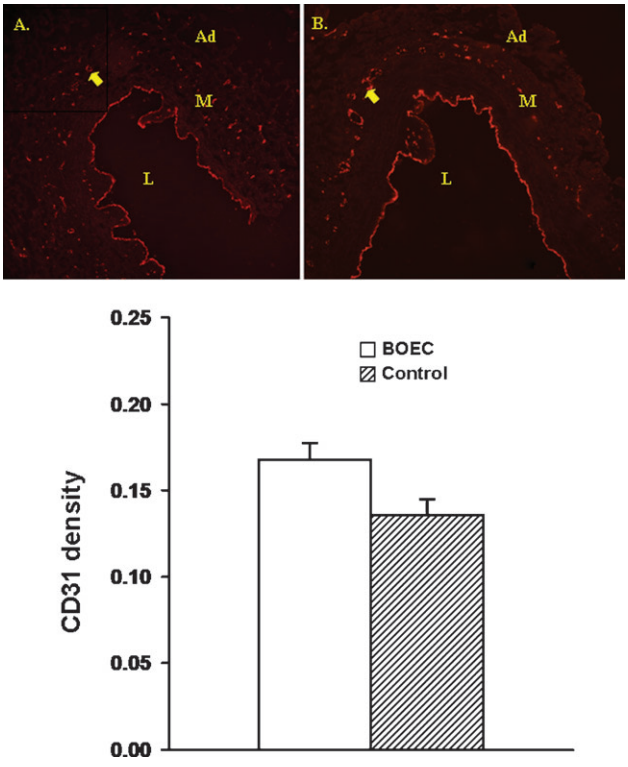

Fig. 7. Indirect immunofluorescence for CD31-positive cells was performed at the venous stenosis from BOEC grafted (**A**) and control specimens (**B**). Ad is adventitia, M is the media and L is the lumen, and the yellow arrow shows microvessel formation. Lower panel shows quantitative assessment from the venous stenosis from BOEC and control grafts. There was increased amount of CD31-positive cells in the BOEC samples when compared to the controls.

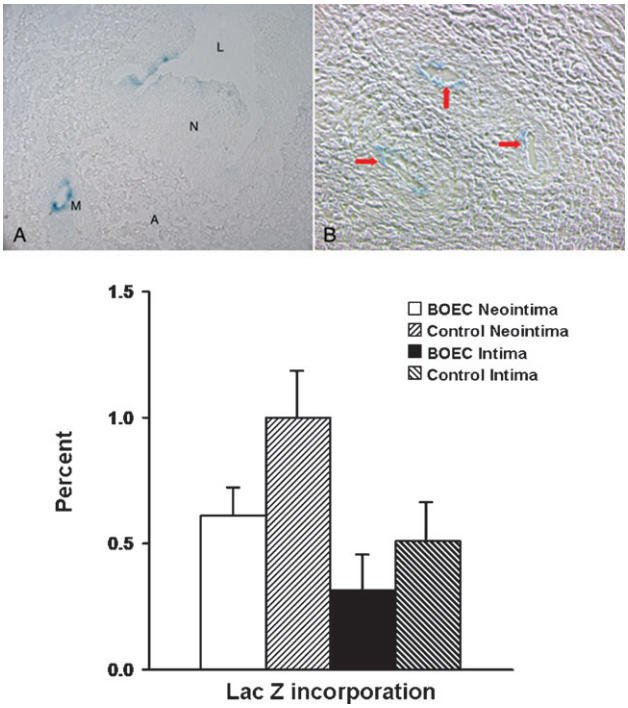

Fig. 8. Staining for β-gal was performed at the vein-to-graft anastomosis removed from the BOEC and contralateral non-transplanted (control) specimens. In (**A**), L is the lumen, N is the neointima, M is a microvessel and A is adventitia. B is a high magnification of the adventitia. (**A**) Engraftment of *Lac Z*-positive labeled BOEC cells (blue) into the neointima (N). In (**B**), there is engraftment of *Lac Z*-positive cells into the microvessel (yellow arrows) in the adventitia. Lower panel shows quantitative analysis of the *Lac Z*-positive BOEC cells into the neointima and intima of both the transplanted and non-transplanted contralateral (control) vein-to-graft anastomosis. There was an increase in the engraftment of *Lac Z*-positive cells into the neointima of the control vein-to-graft anastomosis when compared to the BOEC.

which cells in the venous adventitia can readily enter the systemic circulation (Figure 10).

Discussion

The mechanisms underlying the progression of venous stenosis in patients with haemodialysis vascular access grafts have not been well defined but are felt due to multiple factors, including changes in haemodynamic parameters that include wall shear stress and physiologic changes due to mixing of oxygenated and deoxygenated blood resulting in local vessel hypoxia [5]. Angiogenesis has been observed at sites of intimal hyperplasia in clinical and experimental studies. Hypoxia activates several cytokines that are implicated in the angiogenic process and recently has been shown to be associated with haemodialysis graft failure [6]. In the present paper, we showed that hypoxia causes BOEC to increase the production of both pro MMP-2 and TIMP-2. Adventitial transplantation of BOEC to the vein-to-graft anastomosis at the time of haemodialysis graft placement had several important effects on the BOEC-transplanted vessels: (1) significant reduction in neointimal hyperplasia, (2) a significant reduction in tissue expression of HIF-1α, (3) a significant increase in pro and active MMP-9 activity, (4) enhancement of adventitial angiogenesis and (5) engraftment of BOEC to adventitial microvessels.

Hypoxia is a fundamental stimulus for angiogenesis. It has been shown to mediate gene expression of several important angiogenic factors through increased expression of HIF-1α including VEGF-A, VEGFR-1, MMP-2 and others [5]. All of these proteins have been hypothesized to cause haemodialysis graft failure. A recent study from our laboratory showed that there was significantly increased expression of HIF-1α in tissue removed from the venous stenosis when compared to control veins in a porcine model [6]. Moreover, in clinical specimens removed from patients with PTFE haemodialysis grafts, there was significantly increased expression of HIF-1α when compared to control veins [7]. In the present study, we investigated the role of hypoxia on protein production by BOEC and showed that under hypoxic conditions, BOEC increased the production of both pro MMP-2 by 12 h and TIMP-2 by 24 h when compared to normoxic conditions. Increased up regulation of TIMP-2 has been shown to decrease cell invasion [26]. Several *in vitro* studies have demonstrated increased expression of active MMP-9, by endothelial cells in response to inflammatory cytokines [27], oscillatory shear stress [28], by smooth muscle cells in response to cytokines [29] and constitutively by inflammatory cells [30].

Multiple investigators have shown that circulating bone marrow-derived progenitor cells functionally contribute to

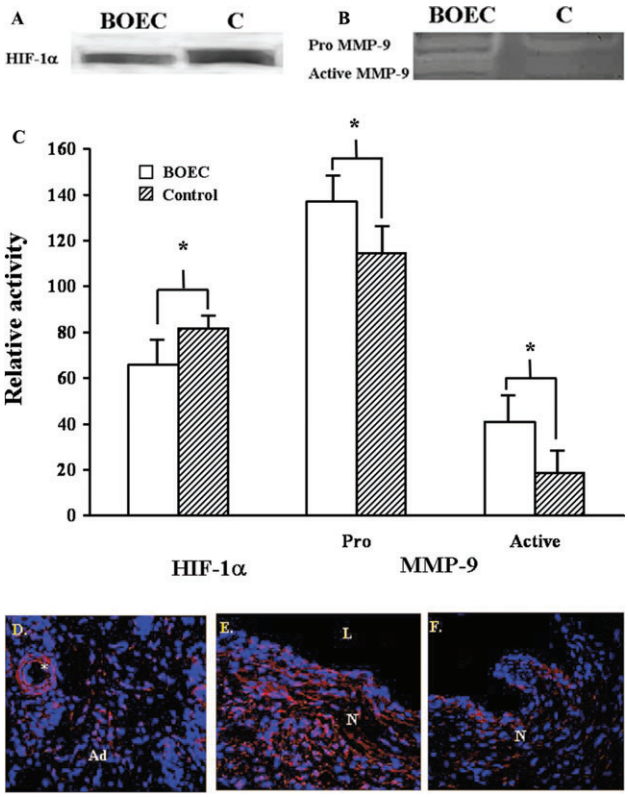

Fig. 9. Graph representing appropriate protein band HIF-1α (**A**) from western blot analysis and pro and active MMP-9 from zymography (**B**) with blood outgrowth endothelial cell (BOEC) delivery compared to control (**C**). According to semiquantitative analysis, by Day 14, the normalized density of HIF-1α was significantly less in the BOEC samples when compared to control ($P < 0.05$) while the normalized density of both pro and active MMP-9 was significantly higher than the control vessels ($P < 0.05$). (**D**), (**E**) Confocal double immunostaining of MMP-9-positive cells (red) from BOEC-transplanted vessels and (**F**) the contralateral non-transplanted (control) vessel. Ad is the adventitia, M is the media, N is the neointima and L is the lumen. *An adventitial microvessel surrounded by cells expressing MMP-9. More intense immunostaining was observed in the neointima of the transplanted vessels when compared to non-transplanted vessels.

angiogenesis during hypoxic pathology such as limb ischemia [31] and myocardial infarction [32]. However, few investigators have targeted the adventitia directly. Targeting the adventitia is technically easier because BOEC can be transplanted to the site of injury without significant washout of cells, as can occur with intraluminal delivery. This technique has many benefits and can be expanded to other experimental vascular injury models such as vein bypass grafts used as arterial conduits, arterial restenosis after angioplasty and stent placement, and atherosclerosis in which the adventitia has been implicated in neointima formation. Transplantation of BOEC was performed by a unique method to promote engraftment of the progenitor cells by using biodegradable nanopore scaffolding wrapped around the adventitia of the vein-to-graft anastomosis at the time of graft placement resulting in a significant decrease in HIF-1α in the transplanted vessels when compared to control vessels.

The changes in protein expression in BOEC-transplanted vessels suggest several potential mechanisms by which BOEC may have promoted favorable venous remodeling. A significant increase in the expression of both pro and active MMP-9 was observed in the BOEC-transplanted vessels when compared to control vessels. Previous work from this laboratory in both a rat and a porcine model of haemodialysis grafts has shown no evidence of active MMP-9 in venous stenosis formation [9,19] and in clinical specimens as well [7]. Furthermore, no active MMP-9 was observed in venous stenotic tissue removed from animals with bilateral PTFE grafts with scaffolding and virus alone (no BOEC), suggesting that the presence of active MMP-9 was due to the transplantation of BOEC and not the scaffolding. Immunohistochemistry of the BOEC-transplanted vessel localized MMP-9 to the adventitia, media and neointima with the highest expression in the neointima. Given the low degree of incorporation of *Lac Z*-positive cells into the adventitia (<1%) and neointima (1–2%), these findings suggest that BOEC may act through a paracrine mechanism to upregulate the expression of MMP-9 and conversion to its active form.

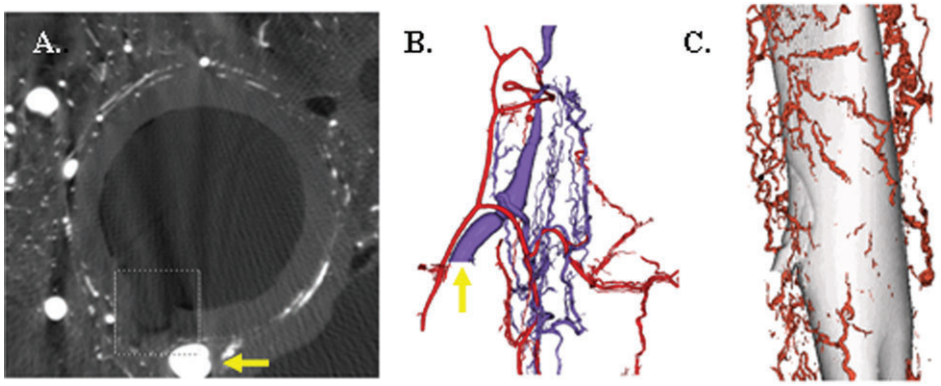

Fig. 10. Three-dimensional microscopic computed tomographic evaluation of the carotid artery and jugular vein. (**A**) A pig carotid artery cross section showing the lumen and the origin of a vasa vasorum externa with microfilm (box). Yellow arrow is shown in (**B**). (**B**) The arterial vasa vasorum (red) and the venous vasa vasorum (blue) with the yellow arrow on the vasa vasorum from (**A**). (**C**) The vasa vasorum surrounding the vein that communicates with the arterial vasa vasorum.

It has been shown recently that adventitial fibroblasts will convert to myofibroblasts and migrate into the neointima contributing to venous stenosis formation [9,23]. Furthermore, it has been shown in fibroblasts harvested from the pulmonary artery, that hypoxia will stimulate the conversion of fibroblasts to myofibroblasts [33]. It is possible that the BOEC may have acted on fibroblasts by decreasing the conversion of fibroblasts to myofibroblasts through a MMP-2/TIMP-2-mediated pathway. Recently, it has been shown that increased TIMP-2 will decrease the ability of cells to invade in breast carcinoma [26]. Further experiments need to be performed to confirm this hypothesis.

Active MMP-9 has been suggested to be the key mediator in the angiogenic switch [34], a term used to describe the transition from an avascular tumour to an angiogenic phenotype [35]. MMP-9 has been shown to have a role in capillary branching and is required for adequate angiogenic revascularization of ischaemic tissue [36]. Activation of MMP-9 increases the bioavailability of VEGF-A [34] through direct cleavage of VEGF-A, releasing it from its matrix-binding motif and converting it to the soluble form [37]. In the present study, despite increased adventitial angiogenesis in the BOEC-transplanted vessels, no significant elevations in VEGF-A were seen. The VEGF-A detected by Western blot analysis is likely matrix-bound VEGF-A rather than the soluble form. Increased levels of active MMP-9 may have increased the conversion of VEGF-A from the matrix bound form to soluble form and therefore may not be detected. Alternatively, VEGF-A levels may have peaked at an earlier time point or other angiogenic factors may have been involved. These findings suggest a possible MMP-9-mediated mechanism by which BOEC promotes angiogenesis.

MMP-9 has been shown to play a role in aneurysmal formation through active secretion by smooth muscle cells and macrophages [38]. There was minimal inflammation observed at the vein-to-graft anastomosis with the exception of a rare macrophage seen in the adventitia adjacent to degraded scaffolding. No evidence of aneurysm formation was observed by MRI and there was no difference in medial thickness between the BOEC-transplanted vessel and the contralateral non-transplanted (control) vessels. This suggests that the changes seen in luminal vessel area were a result of a decrease in neointima formation but not from aneurysmal formation.

A trend toward increased angiogenesis was observed in BOEC-transplanted vessels with engraftment of *Lac Z*-positive BOEC into the adventitial microvasculature at 2 weeks. Additionally, *Lac Z*-positive BOEC were present in the neointima of both the ipsilateral transplanted BOEC vessels and contralateral non-transplanted (control) vessels, but no *Lac Z*-positive cells were visualized within the media. It is possible that migration of the *Lac Z*-positive BOEC into the media may have occurred prior to the 2 weeks. Alternatively, BOEC may have entered the systemic circulation via the vasa vasorum that communicates between the carotid artery and external jugular vein as demonstrated by the three-dimensional microscopic computed tomographic analysis.

The degree of BOEC engraftment in the neointima was greater in the non-transplanted vessels in which tissue levels of HIF-1α were also increased. A recent study demonstrated that HIF-1α up-regulated the expression of chemokine stromal cell-derived factor-1 (SDF-1) that increased the adhesion, migration and homing of circulating progenitor cells to ischaemic tissue [39]. Interestingly, SDF-1 and MMP-9 have been shown to be involved in cell homing [40]. The results of the present study suggest that homing and engraftment of BOEC to neointima may be regulated through the elevated HIF-1α levels and hypoxia. However, other mechanisms mediated through SDF-1 may play a role in cell homing.

In conclusion, our study provides evidence to suggest that transplantation of BOEC to the adventitia of vein-to-graft anastomosis of haemodialysis grafts reduces venous stenosis formation. There was a decrease in HIF-1α suggesting alleviation of hypoxia and increased production of active and pro MMP-9 suggesting a possible mechanism by which BOEC may enhance angiogenesis. Additional experiments need to be performed to confirm these observations as well as the durability of these early results. Adventitial targeting has many potential therapeutic applications in cell-based gene therapy and can be expanded to other experimental vascular injury models including vein bypass grafts, arterial restenosis after angioplasty and stent placement, and atherosclerosis.

Limitations

The aim of the present study was to examine the effects of adventitial delivery on haemodialysis graft remodeling. Examination of protein expression focused on basic factors known to play a role in angiogenesis and smooth muscle cell migration. However, there are many other potential cytokines and haemodynamic stimuli that contribute to these processes. The contribution of these to venous stenosis in our model is currently under investigation. Additionally, the current study was not designed to examine the effects of BOEC engraftment to the neointima as this was somewhat of an unexpected finding. Whether BOEC engraftment to the neointima promotes or attenuates the progression of neointima formation remains unclear and will need to be addressed in future studies. Finally, the durability of the observed results is unknown because of the short duration the animals were followed.

Acknowledgements. The authors would like to thank Dr Eric Ritman for his help with the three-dimensional microscopic computed tomographic analysis. A portion of this work is partially supported by his NIH grant HL 65342. This work is also supported by NIH grants CA78383, HL072178 and HL70567 and also a grant from American Cancer Society to D.M. D.B. is a Mayo Clinic CI fellow. The authors would also like to thank Jill L. Anderson and Steve Krage for their help with the animal experiments, Tanya Hoskin for her help with the statistical analysis and Dr Kallmes for the use of his laboratory.

Conflict of interest statement. None declared.

References

1. Collins AJ, Kasiske B, Herzog C *et al*. Excerpts from the United States renal data system 2003 annual data report: atlas of end-stage renal disease in the United States. *Am J Kidney Dis*. 2003; 42(Suppl 5): A5–A7

2. Schwab SJ, Harrington JT, Singh A *et al*. Vascular access for haemodialysis. *Kidney Int* 1999; 55: 2078–2090
3. Sullivan KL, Besarab A, Bonn J *et al*. Haemodynamics of failing dialysis grafts. *Radiology* 1993; 186: 867–872
4. Roy-Chaudhury P, Kelly BS, Miller MA *et al*. Venous neointimal hyperplasia in polytetrafluoroethylene dialysis grafts. *Kidney Int* 2001; 59: 2325–2334
5. Semenza GL. Targeting HIF-1 for cancer therapy. *Nat Rev Cancer* 2003; 3: 721–732
6. Misra S, Fu A, Pugionni A *et al*. Increased expression of hypoxia inducible factor-1α in a porcine model of chronic renal insufficiency with arteriovenous polytetrafluoroethylene grafts. *J Vasc Interv Radiol* 2008; 19: 260–265
7. Misra S, Fu A, Rajan D *et al*. Expression of hypoxia inducible factor-1 alpha, macrophage migration inhibition factor, matrix metalloproteinase-2 and -9, and their inhibitors in haemodialysis grafts and arteriovenous fistulas. *J Vasc Interv Radiol* 2008; 19: 252–259
8. Hueper WC. Atherosclerosis: the anoxemia theory. *Arch Pathol* 1944; 28: 173–205
9. Misra S, Doherty MG, Woodrum D *et al*. Adventitial remodeling with increased matrix metalloproteinase-2 activity in a porcine arteriovenous polytetrafluoroethylene grafts. *Kidney Int* 2005; 68: 2890–2900
10. Rundhaug JE. Matrix metalloproteinases and angiogenesis. *J Cell Mol Med* 2005; 9: 267–285
11. Rotmans JI, Velema E, Verhagen HJ *et al*. Matrix metalloproteinase inhibition reduces intimal hyperplasia in a porcine arteriovenous-graft model. *J Vasc Surg* 2004; 39: 432–439
12. Westerweel PE, Hoefer IE, Blankestijn PJ *et al*. End-stage renal disease causes an imbalance between endothelial and smooth muscle progenitor cells. *Am J Physiol Renal Physiol* 2007; 292: F1132–F1140
13. Baigent C, Burbury K, Wheeler D. Premature cardiovascular disease in chronic renal failure. *Lancet* 2000; 356: 147–152
14. Gulati R, Jevremovic D, Peterson TE *et al*. Autologous culture-modified mononuclear cells confer vascular protection after arterial injury. *Circulation* 2003; 108: 1520–1526
15. Gulati R, Lerman A, Simari RD. Therapeutic uses of autologous endothelial cells for vascular disease. *Clin Sci (Lond)* 2005; 109: 27–37
16. Yoon C-H, Hur J, Park K-W *et al*. Synergistic neovascularization by mixed transplantation of early endothelial progenitor cells and late outgrowth endothelial cells: the role of angiogenic cytokines and matrix metalloproteinases. *Circulation* 2005; 112: 1618–1627
17. Misra S, Gordon JD, Fu AA *et al*. The porcine remnant kidney model of chronic renal insufficiency. *J Surg Res* 2006; 135: 370–379
18. Lin Y, Weisdorf DJ, Solovey A *et al*. Origins of circulating endothelial cells and endothelial outgrowth from blood. *J Clin Invest* 2000; 105: 71–77
19. Misra S, Fu A, Anderson J *et al*. The rat femoral arteriovenous fistula model: Increased expression of MMP-2 and MMP-9 at the venous stenosis. *J Vasc Interv Radiol* 2008; 19: 587–594
20. Misra S, Fu AA, Puggioni A *et al*. Increased shear stress with up regulation of VEGF-A and its receptors and MMP-2, MMP-9, and TIMP-1 in venous stenosis of haemodialysis grafts. *Am J Physiol Heart Circ Physiol* 2008; 294: H2219–H2230
21. Godbey WT, Hindy SB, Sherman ME *et al*. A novel use of centrifugal force for cell seeding into porous scaffolds. *Biomaterials* 2004; 25: 2799–2805
22. Misra S, Woodrum D, Homburger J *et al*. Assessment of wall shear stress changes in arteries and veins of arteriovenous polytetrafluoroethylene grafts using magnetic resonance imaging. *Cardiovasc Intervent Radiol* 2006; 29: 624–629
23. Wang Y, Krishnamoorthy M, Banerjee R *et al*. Venous stenosis in a pig arteriovenous fistula model anatomy, mechanisms and cellular phenotypes. *Nephrol Dial Transplant* 2007; 22: 3139–3146
24. Jorgensen S, Demirkaya O, Ritman E. Three dimensional imaging of vasculature and parenchyma in intact rodent organs with x-ray micro-CT. *Am J Physiol Heart Circ Physiol* 1998; 275: H1103–H1114
25. Goessl M, Rosol M, Malyar N *et al*. Functional anatomy and haemodynamic characteristics of vasa vasorum in the walls of porcine coronary arteries. The anatomical record (Part A). *Anat Rec A Discov Mol Cell Evol Biol* 2003; 272: 526–537
26. Simeone AM, McMurtry V, Nieves-Alicea R *et al*. TIMP-2 mediates the anti-invasive effects of the nitric oxide-releasing prodrug JS-K in breast cancer cells. *Breast Cancer Res* 2008; 10: R44
27. Jackson CJ, Nguyen M. Human microvascular endothelial cells differ from macrovascular endothelial cells in their expression of matrix metalloproteinases. *Int J Biochem Cell Biol* 1997; 29: 1167–1177
28. Magid R, Murphy TJ, Galis ZS. Expression of matrix metalloproteinase-9 in endothelial cells is differentially regulated by shear stress. Role of c-Myc. *J Biol Chem* 2003; 278: 32994–32999
29. Galis ZS, Muszynski M, Sukhova GK *et al*. Cytokine-stimulated human vascular smooth muscle cells synthesize a complement of enzymes required for extracellular matrix digestion. *Circ Res* 1994; 75: 181–189
30. Hanemaaijer R, Koolwijk P, le Clercq L *et al*. Regulation of matrix metalloproteinase expression in human vein and microvascular endothelial cells. Effects of tumour necrosis factor alpha, interleukin 1 and phorbol ester. *J Biochem* 1993; 296(Pt 3): 803–809
31. Asahara T, Murohara T, Sullivan A *et al*. Isolation of putative progenitor endothelial cells for angiogenesis. *Science* 1997; 275: 964–967
32. Orlic D, Kajstura J, Chimenti S *et al*. Bone marrow cells regenerate infarcted myocardium. *Nature* 2001; 410: 701–705
33. Das M, Burns N, Wilson SJ *et al*. Hypoxia exposure induces the emergence of fibroblasts lacking replication repressor signals of PKC{zeta} in the pulmonary artery adventitia. *Cardiovasc Res* 2008; 78: 440–448
34. Bergers G, Brekken R, McMahon G *et al*. Matrix metalloproteinase-9 triggers the angiogenic switch during carcinogenesis. *Nat Cell Biol* 2000; 2: 737–744
35. Hanahan D, Folkman J. Patterns and emerging mechanisms of the angiogenic switch during tumorigenesis. *Cell* 1996; 86: 353–364
36. Johnson C, Sung HJ, Lessner SM *et al*. Matrix metalloproteinase-9 is required for adequate angiogenic revascularization of ischaemic tissues: potential role in capillary branching. *Circ Res* 2004; 94: 262–268
37. Lee S, Jilani SM, Nikolova GV *et al*. Processing of VEGF-A by matrix metalloproteinases regulates bioavailability and vascular patterning in tumors. *J Cell Biol* 2005; 169: 681–691
38. Pasterkamp G, Galis ZS, de Kleijn DP. Expansive arterial remodeling: location, location, location. *Arterioscler Thromb Vasc Biol* 2004; 24: 650–657
39. Ceradini DJ, Kulkarni AR, Callaghan MJ *et al*. Progenitor cell trafficking is regulated by hypoxic gradients through HIF-1 induction of SDF-1. *Nat Cell Biol* 2004; 10: 858–864
40. Kollet O, Shivtiel S, Chen Y-Q *et al*. HGF, SDF-1, and MMP-9 are involved in stress-induced human CD34+ stem cell recruitment to the liver. *J Clin Invest* 2003; 112: 160–169

Received for publication: 18.2.08
Accepted in revised form: 7.7.08